Nanorods

DOI: 10.1002/anie.201004910

The Crystalline Structure of Gold Nanorods Revisited: Evidence for Higher-Index Lateral Facets**

*Enrique Carbó-Argibay, Benito Rodríguez-González, Sergio Gómez-Graña, Andrés Guerrero-Martínez, Isabel Pastoriza-Santos, Jorge Pérez-Juste, and Luis M. Liz-Marzán**

Gold nanorods (GNRs) have become one of the most widely studied types of nanoparticles. The main reason for this is their well-defined anisotropy, which greatly influences various properties, among which the optical extinction can be singled out.[1] Gold NRs display two separate localized surface plasmon resonances in the visible/near-IR spectral range, due to transverse and longitudinal oscillations of conduction electrons. In particular, the longitudinal plasmon bands have extremely high extinction cross sections and can be tuned through the aspect ratio of the GNRs, thus giving rise to a number of interesting applications in fields as diverse as biomedicine[2,3] or information storage.[4] Interestingly, chemical methods for the growth of GNRs have been optimized in such a way that mass production with high yields can be achieved.[5,6] The most popular synthesis method is undoubtedly the seed-mediated growth in aqueous solution, assisted by a surfactant and Ag^+ ions.[7,8] In this method, small gold seeds are prepared by reduction of $HAuCl_4$ with $NaBH_4$ in the presence of the surfactant cetyltrimethylammonium bromide (CTAB), and subsequently added to a growth solution containing additional $HAuCl_4$, Ag^+, and CTAB, as well as ascorbic acid as a weak reducing agent, which results in anisotropic growth on the initial, single-crystal seeds. The classical description of this growth is based on the formation of single-crystal GNRs with a $<001>$ longitudinal growth direction.[9] Wang et al. carried out a detailed electron microscopy study to elucidate the crystalline structure of GNRs, which seemed to indicate formation of nanocrystals with an octagonal cross section, bound by alternate {100} and {110} facets that would converge at the tips in the form of {110} and {111} facets, respectively.[9] Although this analysis was carried out on nanorods synthesized electrochemically, it was assumed that it holds for those obtained by seeded chemical growth. Such a description would imply that the actual areas of the two types of lateral facets are not equal but the angles between them are all equivalent. However, the proposed assignment is not the only possible interpretation of their analysis, as specifically indicated in reference [9], because the study was carried out on GNRs lying flat on the TEM grid, so that not all of the different orientations of the nanocrystals could be probed.

Here we present new pieces of evidence indicating that the assignment of Wang et al. is actually incorrect, and thus many of the interpretations regarding the growth, reactivity, and adsorption properties of GNRs must be revisited. The key to obtaining this new information was the capability of analyzing GNRs that stand perpendicular to the substrate, so that the different orientations and crystallographic directions can be properly distinguished. Therefore, the GNRs used for the data presented here were grown by replacing CTAB (during GNR growth) by a gemini surfactant, as recently reported,[10] which helps to obtain self-assembled, standing GNRs. Moreover, we confirmed that this analysis is also common to the usual CTAB GNRs. When standing GNRs were imaged by high-resolution TEM (HRTEM), their octagonal cross section was readily identified, as shown in the example selected for Figure 1 and in many others (see Figure S2 in Supporting Information).

Despite the thickness traversed by the electron beam through the GNRs (ca. 50 nm), close inspection of all the images in Figure 1 and Figure S2 (Supporting Information) shows the lattice spacing of face-centered cubic (fcc) gold, that is, the particles are indeed single crystals. Thus, we analyzed the fast Fourier transform (FFT) obtained from each of these images. In all cases we could invariably assign the [001] zone axis, in agreement with the growth direction indicated by Wang et al.[9] Additionally, we obtained a set of spots in the FFT that allowed assignment of the crystallographic directions for the sides and corners, as shown in Figure 1 and Figure S2 (Supporting Information). It is clear from this image that the $<100>$ and $<110>$ directions are always in coincidence with corners, whereas the $<250>$ directions point toward the lateral facets. An example of the method used for the assignment is shown in Figure 2. The fcc gold reciprocal lattice spot pattern, projected in the $<001>$ zone axis, was overlapped and aligned with the FFT of the HRTEM image, and indexation was carried out by drawing direction vectors perpendicular to the corresponding facets. Although these results are clearly in conflict with the assignment that has been accepted so far, they are still consistent with the analysis made by Wang et al.,[9] as shown in Figure 3. This actually indicates that all lateral facets are in fact higher-index ({250}) facets, and they all have equal surface area (Figure S3, Supporting Information). Correspondingly, the tip facets would all be of {111} and {110} types

[*] E. Carbó-Argibay, Dr. B. Rodríguez-González, S. Gómez-Graña, Dr. A. Guerrero-Martínez, Dr. I. Pastoriza-Santos, Dr. J. Pérez-Juste, Prof. L. M. Liz-Marzán
Departamento de Quimica Fisica and
Unidad Asociada CSIC-Universidade de Vigo, 36310 Vigo (Spain)
Fax: (+34) 986-812-556
E-mail: lmarzan@uvigo.es

[**] E.C.-A. and A.G.-M. acknowledge FPU and JdlC fellowships from the Spanish Ministerio de Ciencia e Innovación. This work was funded by MiCInn/FEDER (MAT2007-62696) and Xunta de Galicia (09TMT011314PR).

Supporting information for this article is available on the WWW under http://dx.doi.org/10.1002/anie.201004910.

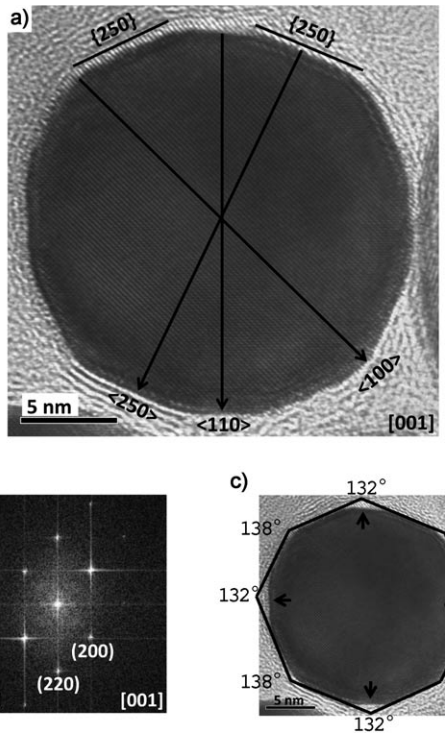

Figure 1. a) HRTEM image of a standing gold nanorod, showing the main crystallographic directions and the indexes of the facets. b) Corresponding FFT spot pattern demonstrating the [001] zone axis. c) Measured angles between lateral facets showing the approximate alternation of angles; the arrows point to $<110>$-type directions, where small bevels can be seen.

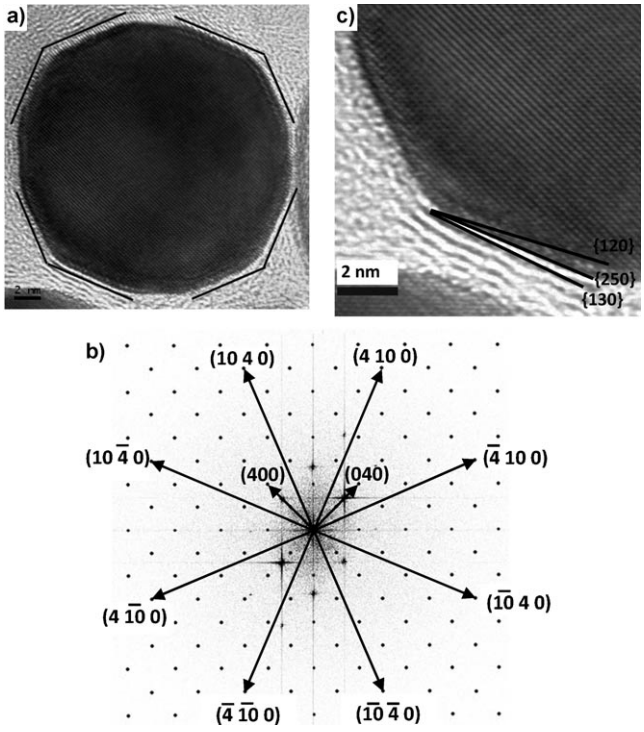

Figure 2. Method used to calculate the index of the side facets. Lines drawn in (a) are perpendiculars to the (4 10 0) direction vectors drawn in (b). c) Comparison of the agreement achieved with {120}-, {130}-, and {250}-type facets.

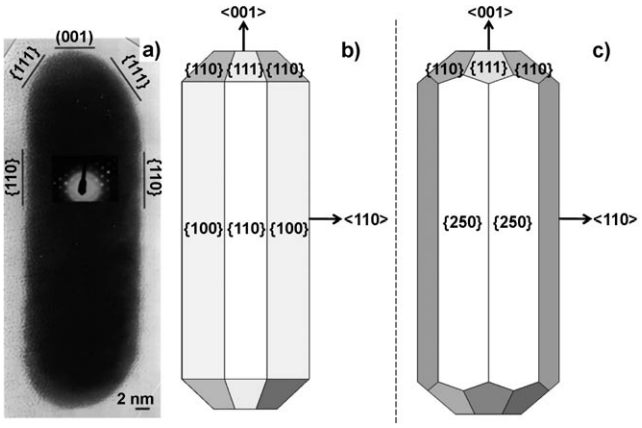

Figure 3. Comparison of Wang and co-workers' analysis (a) and model (b) with the new proposed model (c). Both models are consistent with the TEM analysis. The TEM image in a) was adapted from Ref. [9] with permission from Elsevier.

(see Figure 3 and Figures S4 and S5 of the Supporting Information). Another strong indication that supports the proposed model is based on the measured angles between facets. As can be seen in Figure 1c, these angles show alternating values, between 131–132° and 138–139°. Despite some variations from rod to rod, averaging the angles measured on several rods yielded average values of 134° for the $<110>$ direction and 138° for the $<100>$ direction, in reasonable agreement with the theoretical values of 133.6 and 136.4°, respectively (see Figure S3 and Table S1, Supporting Information). The difference between the measured value and the theoretical model can be attributed to the presence of small bevels at $<110>$ directions and to the rounded edges that connect the facets due to surface tension.[11] In fact, this rounding hinders the assignment of the lateral facets, which could also be interpreted as {130} or {120} (see comparison in Figure 2c and Figure S6, Supporting Information). However, our experimental data strongly support the model with {250} facets, as shown in Figure 2c.

A first consequence of this different crystallographic structure is related to the growth mechanism. Although the selective adsorption of CTAB on {100} facets was initially proposed as the shape-directing factor,[12] it has been repeatedly demonstrated that the presence of Ag^+ ions during the growth step is essential to obtain a high yield of nanorods. This indicates that Ag^+ ions strongly affect the growth rate of different crystallographic facets, which has been explained through the so-called underpotential deposition (UPD) of metallic silver on the different crystal facets of gold,[13,14] and leads to symmetry breaking and rod formation.[15] It has been concluded that the UPD shifts of silver on gold surfaces decrease in the order $\{110\}>\{100\}>\{111\}$, and lead to different growth rates of the simple fcc Au facets, which decrease from the close-packed {111} to higher-energy {100} and {110} surfaces. Following the same argument, the {250} facets, with even higher surface energy, display a more open and accessible structure that would be more favorable for silver deposition, as shown in Figure 4. If all lateral faces are

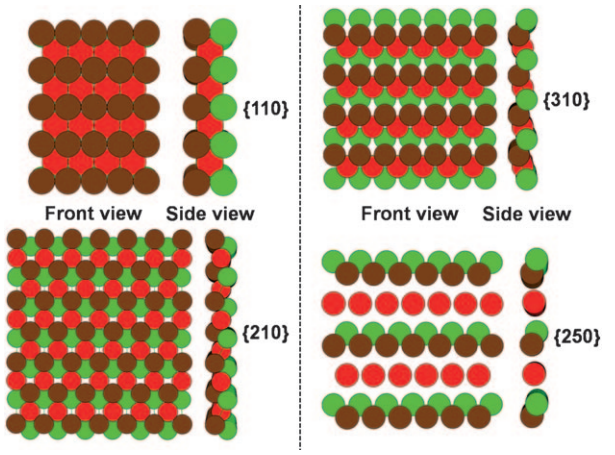

Figure 4. Representation of the first three atomic layers (front and side views) at {110}, {210}, {310}, and {250} facets, showing how the structure becomes more open as the indexes get higher. Colors indicate different atomic layers (brown: top; red: intermediate; green: lower).

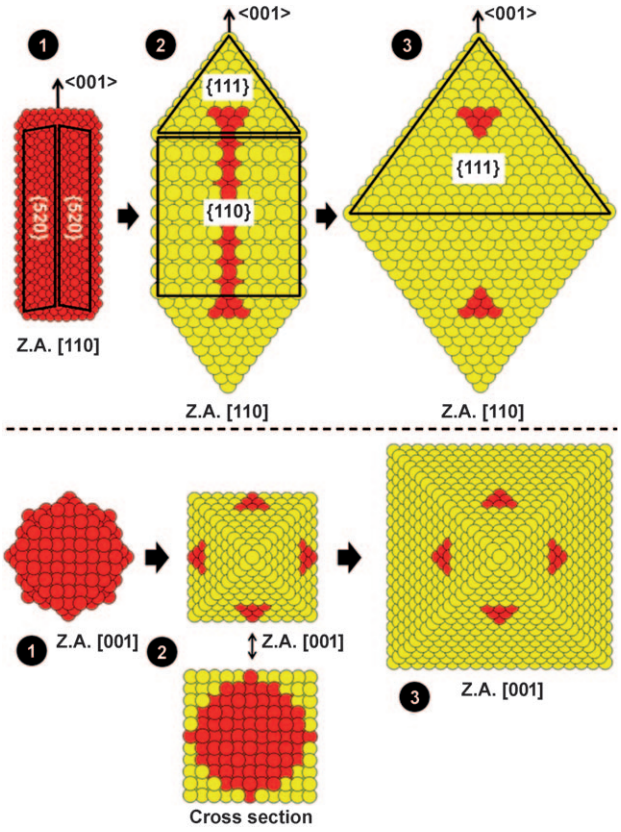

Figure 5. Ball depiction (front and top view) demonstrating a plausible growth model between the new structure proposed for single-crystal gold nanorods, intermediate rods with square cross section, and octahedra, formed by growth in PVP/DMF.[17] High-order {250} lateral facets are less stable than {111} and {110} tip facets and thus grow faster, yielding rods with four {110} lateral facets and four {111} facets in each tip. Z.A. = zone axis.

of {250} type, this mechanism makes even better sense, since the growth rate is uniformly decreased and the symmetry favors one-dimensional growth. Additionally, one could wonder why this system would prefer to expose such high-index facets, so that the surface energy is actually higher. In fact, this could be related to the single-crystalline structure of the particles. Gold nanoparticles show a high tendency to develop stacking faults and twin planes, which has often been reported in pentatwinned decahedra, for example.[16] Twin planes have been shown to decrease the stress derived from the single-crystalline structure of each twin. In single-crystalline nanorods, the absence of twin planes may be compensated by exhibiting more open surfaces which allow greater structural flexibility, and even rounding of the facets, as observed here (see Figure 1 and Figure S2, Supporting Information). This can also explain the relatively low thermal stability of GNRs and easy reshaping into more spherical shapes at mild temperatures.[1]

Another example for which the original GNR structure was difficult to fit to experimental observations is the seeded growth of preformed GNRs through reduction of gold ions in *N*,*N*-dimethylformamide (DMF)/poly(*N*-vinylpyrrolidone) (PVP) solutions.[17] This process was found to ultimately lead to single-crystalline octahedra via intermediate shapes including rods with square cross section. Since the four facets of this intermediate structure were unequivocally assigned to {110} faces, it was thought that gold ions were preferentially reduced on {100} facets, which were thereby exhausted, leaving only the initial {110} at the four new lateral sides. This argument, however, did not correlate well with the relative surface energies, which would indicate the opposite trend. Therefore, it was proposed that adsorption of the polymer (PVP) would lead to reversal of the actual surface energies, but no evidence could be provided to support this statement. With the new crystallographic structure at hand, there is actually no need to make unfounded assumptions, since the {250} facets are of higher energy than the {111} and {110} tip facets, and therefore grow faster (all at the same rate) until they fill the open gap, giving the final structure bound by {110} facets, as schematically shown in Figure 5.

In summary, we have demonstrated that single-crystalline gold nanorods prepared by silver-assisted seeded growth in solution are enclosed by eight identical high-index crystalline facets. Our HRTEM analysis on standing nanorods provided clear evidence that the $<100>$ and $<110>$ crystallographic directions point toward lateral edges, and thus the faces joining on them must be assigned to higher indexes, which appear to be of {250} type. Apart from the relevance of these results for understanding the mechanisms involved in the formation and further growth of these nanoparticles, the findings reported here are important to understand the adsorption of different types of molecules, which often occurs selectively at the tips,[18,19] but can also motivate catalytic studies that often require the availability of higher-index facets with more defect sites and better selectivity for certain reactions.[20,22]

Experimental Section

The gemini surfactant Br^{-}-n-$C_{16}H_{33}NMe_2^{+}$–$CH_2(CH_2OCH_2)CH_2$–$N^{+}Me_2$-n-$C_{16}H_{33}Br^{-}$ (16-EO_1-16) was synthesized according to procedures described in the literature.[21] Gold nanorods were prepared by seeded growth[8,10] at 27 °C through reduction of $HAuCl_4$ with ascorbic acid on CTAB-stabilized Au nanoparticle seeds (2–3 nm) in the presence of 16-EO_1-16 (0.05 M), HCl (pH 2–3), and $AgNO_3$ (0.12 mM). After synthesis, the gold nanorod solution (5 mL) was centrifuged twice (8000 rpm, 20 min) to remove excess reactants and to obtain a final concentration of gemini surfactant close to 1 mM.

HRTEM analysis was carried out in a JEOL JEM 2010 FEG TEM operating at an acceleration voltage of 200 KV. A double-tilt holder was employed to orient each nanorod in the [001] zone axis. The HRTEM images of the cross section of gold nanorods were acquired with the nanorod oriented in the [001] zone axis. The specimens were prepared by depositing a droplet on pure carbon-coated grids and evaporating the solvent in air at room temperature. A plasma cleaner (with a mixture of H_2 and O_2) was used to remove organics and clean the sample for HRTEM analysis. Before aligning the nanorod in the [001] zone axis, we confirmed that the analyzed particle was a real rod by tilting the microscope holder (see Figure S1, Supporting Information).

Received: August 6, 2010
Published online: November 4, 2010

Keywords: crystal growth · electron microscopy · gold · nanostructures · solid-state structures

[1] J. Pérez-Juste, I. Pastoriza-Santos, L. M. Liz-Marzán, P. Mulvaney, *Coord. Chem. Rev.* **2005**, *249*, 1870 – 1901.
[2] X. Huang, S. Neretina, M. A. El-Sayed, *Adv. Mater.* **2009**, *21*, 4880 – 4910.
[3] C. J. Murphy, A. M. Gole, J. W. Stone, P. N. Sisco, A. M. Alkilany, E. C. Goldsmith, S. C. Baxter, *Acc. Chem. Res.* **2008**, *41*, 1721 – 1730.
[4] P. Zijlstra, J. W. M. Chon, M. Gu, *Nature* **2009**, *459*, 410 – 413.
[5] N. R. Jana, *Small* **2005**, *1*, 875 – 882.
[6] S. Duraiswamy, S. A. Khan, *Small* **2009**, *5*, 2828 – 2834.
[7] N. R. Jana, L. Gearheart, C. J. Murphy, *Adv. Mater.* **2001**, *13*, 1389 – 1394.
[8] B. Nikoobakht, M. A. El-Sayed, *Chem. Mater.* **2003**, *15*, 1957 – 1962.
[9] Z. L. Wang, M. B. Mohamed, S. Link, M. A. El-Sayed, *Surf. Sci.* **1999**, *440*, L809 – L814.
[10] A. Guerrero-Martínez, J. Pérez-Juste, E. Carbó-Argibay, G. Tardajos, L. M. Liz-Marzán, *Angew. Chem.* **2009**, *121*, 9648 – 9652; *Angew. Chem. Int. Ed.* **2009**, *48*, 9484 – 9488.
[11] A. A. Golovin, S. H. Davis, A. A. Nepomnyashchy, *Phys. D* **1998** *122*, 202 – 230.
[12] C. J. Johnson, E. Dujardin, S. A. Davis, C. J. Murphy, S. Mann, *J. Mater. Chem.* **2002**, *12*, 1765 – 1770.
[13] M. Liu, P. Guyot-Sionnest, *J. Phys. Chem. B* **2005**, *109*, 22192 – 22200.
[14] M. Grzelczak, J. Pérez-Juste, P. Mulvaney, L. M. Liz-Marzán, *Chem. Soc. Rev.* **2008**, *37*, 1783 – 1791.
[15] F. Giannici, T. Placido, M. L. Curri, M. Striccoli, A. Agostiano, R. Comparelli, *Dalton Trans.* **2009**, 10367 – 10374.
[16] C. L. Johnson, E. Snoeck, M. Excurdia, B. Rodríguez-González, I. Pastoriza-Santos, L. M. Liz-Marzán, M. J. Hÿtch, *Nat. Mater.* **2008**, *7*, 120 – 124.
[17] E. Carbó-Argibay, B. Rodríguez-González, J. Pacifico, I. Pastoriza-Santos, J. Pérez-Juste, L. M. Liz-Marzán, *Angew. Chem.* **2007**, *119*, 9141 – 9145; *Angew. Chem. Int. Ed.* **2007**, *46*, 8983 – 8987.
[18] K. K. Caswell, J. N. Wilson, U. H. F. Bunz, C. J. Murphy, *J. Am. Chem. Soc.* **2003**, *125*, 13914 – 13915.
[19] M. Grzelczak, A. Sánchez-Iglesias, B. Rodríguez-González, R. Alvarez-Puebla, J. Pérez-Juste, L. M. Liz-Marzán, *Adv. Funct. Mater.* **2008**, *18*, 3780 – 3786.
[20] N. Tian, Z.-Y. Zhou, S.-G. Sun, Y. Ding, Z. L. Wang, *Science* **2007**, *316*, 732 – 735.
[21] A. Guerrero-Martínez, G. González-Gaitano, M. H. Viñas, G. Tardajos, *J. Phys. Chem. B* **2006**, *110*, 13819 – 13828.
[22] During the processing of this manuscript, a related paper has been brought to our attention, which is in close agreement with our main conclusion: H. Katz-Boon, C. J. Rossouw, M. Weyland, A. Funston, P. Mulvaney, J. Etheridge, *Nano Lett.* **2010**, in press.

